

## Electronic Supplementary Information

for:

Urchin-like ZnO nanorod arrays for gas sensing applications

*Davide Barreca,<sup>a\*</sup> Daniela Bekermann,<sup>b</sup> Elisabetta Comini,<sup>c</sup> Anjana Devi,<sup>b</sup>  
Roland A. Fischer,<sup>b</sup> Alberto Gasparotto,<sup>d</sup> Chiara Maccato,<sup>d</sup>  
Cinzia Sada,<sup>e</sup> Giorgio Sberveglieri,<sup>c</sup> and Eugenio Tondello<sup>d</sup>*

<sup>a</sup> CNR-ISTM and INSTM - Department of Chemistry - Padova University - 35131 Padova, Italy.

<sup>b</sup> Inorganic Materials Chemistry Group - Lehrstuhl für Anorganische Chemie II -  
Ruhr-University Bochum - 44780 Bochum, Germany.

<sup>c</sup> CNR-IDASC, SENSOR Lab - Department of Chemistry and Physics -  
Brescia University - 25133 Brescia, Italy.

<sup>d</sup> Department of Chemistry - Padova University and INSTM - 35131 Padova, Italy.

<sup>e</sup> Department of Physics and CNISM - Padova University - 35131 Padova, Italy.

\*Corresponding author: Fax: + 39 049 8275161; Tel: + 39 049 8275170; E-mail:  
[davide.barreca@unipd.it](mailto:davide.barreca@unipd.it)

## S1. Synthesis

The substrates used for the fabrication of the present ZnO assemblies were polycrystalline Al<sub>2</sub>O<sub>3</sub> slides (Haldeman & Porret). After cleaning in dichloromethane and rinsing in isopropanol in an ultrasonic bath, the substrates were transferred into a custom-built Radio-Frequency (RF,  $\nu = 13.56$  MHz) PE-CVD system previously described<sup>S1</sup> for ZnO growth. The apparatus, equipped with both rotary and turbo-molecular pumps (Edwards), consisted of a vacuum metal chamber with a first electrode powered by an RF generator (Cesar 133 Thin Films) and a second one electrically grounded, to which the substrates were fixed with metallic clips. In each experiment, the ground electrode was resistively heated and its temperature was measured by a thermocouple. The diameter of each electrode was 9 cm and the inter-electrode distance was fixed at 6 cm. Prior to each deposition, the system was evacuated to a base pressure lower than 10<sup>-5</sup> mbar, as measured by an inverted magnetron gauge (Edwards). Flow rate values were controlled by flow-meters (MKS Instruments) with  $\pm 1$  sccm accuracy, whereas the deposition pressure was monitored by barocel-capacitance manometers (Edwards).

Growth experiments were performed for a total duration of 1 hour at RF-power values of 20 W and temperatures of 200-300°C. The use of lower temperatures was discarded, since preliminary experiments performed at 100°C produced an isotropic ZnO growth, resulting in almost compact layers. The Zn(II) ketoiminate precursor, Zn[(R)NC(CH<sub>3</sub>)=C(H)C(CH<sub>3</sub>)=O]<sub>2</sub>, with R = -(CH<sub>2</sub>)<sub>3</sub>OCH<sub>3</sub>, synthesized according to a recently reported procedure,<sup>S2</sup> was placed in an external vessel heated by an oil bath (140-150°C) and transported towards the deposition zone by an electronic grade Ar flow (rate = 30-60 sccm). Two further auxiliary gas-lines were used to introduce Ar (15 sccm) and electronic grade O<sub>2</sub> (8-20 sccm) directly into the reactor chamber, that was maintained at a working pressure of 0.5-1 mbar. The gas lines connecting the precursor

vessel and reaction chamber were kept at 160°C by means of heating tapes to avoid undesired condensation phenomena.

## S2. Characterization

Glancing incidence X-ray diffraction analyses (GIXRD) were performed by means of a Bruker D8 Advance diffractometer equipped with a Göbel mirror and a CuK $\alpha$  source (40 kV, 40 mA), at a fixed incidence angle of 1.0°.

Fig. S1a evidenced the reflections of the hexagonal ZnO *wurtzite* phase (*zincite*; JCPDS card n° 36–1451), together with three intense diffraction peaks due to the Al<sub>2</sub>O<sub>3</sub> substrate. In both diffractograms, the (002) ZnO signal at  $2\vartheta = 34.4^\circ$  was remarkably more intense than the other reflections ( $2\vartheta = 31.8, 36.3$  and  $47.5^\circ$ , related to the (100), (101) and (102) *zincite* planes, respectively). It is also worthwhile observing that the intensity of zinc oxide diffraction peaks progressively increased with respect to the Al<sub>2</sub>O<sub>3</sub> signals upon increasing the overall ZnO deposit thickness (see caption for Fig. S1).

In order to investigate the in-depth chemical composition of the present specimens, secondary ion mass spectrometry (SIMS) measurements were performed. The analyses were carried out by means of a IMS 4f mass spectrometer (Cameca, Padova, Italy) using a 14.5 KeV Cs<sup>+</sup> primary beam and by negative secondary ion detection. SIMS spectra were recorded at 15 nA primary beam intensity (0.6% stability) rastering over a 175×175  $\mu\text{m}^2$  area and detecting secondary ions from a sub-region close to 10×10  $\mu\text{m}^2$  to avoid crater effects. The signals were collected in beam blanking mode (*i.e.* interrupting the sputtering process during magnet stabilization periods) in order to improve the in-depth resolution, operating in High Mass Resolution configuration to avoid mass interference artefacts. Charge compensation was achieved by means of an electron gun.

As a general rule, the ZnO nanodeposits presented a uniform and parallel Zn and O distribution up to the interface with the substrate (Figs. S1b-c), confirming thus their common chemical origin. For each sample, the erosion speed was evaluated at various depths by measuring the corresponding crater by means of a Tencor Alpha Step profiler. The dependence of the sputtering rate on the material composition was therefore taken into account in the thickness determination. The conversion of the erosion time into thickness was carried out by considering even interdiffusion phenomena, instrumental artefacts and the influence of the alumina surface roughness.

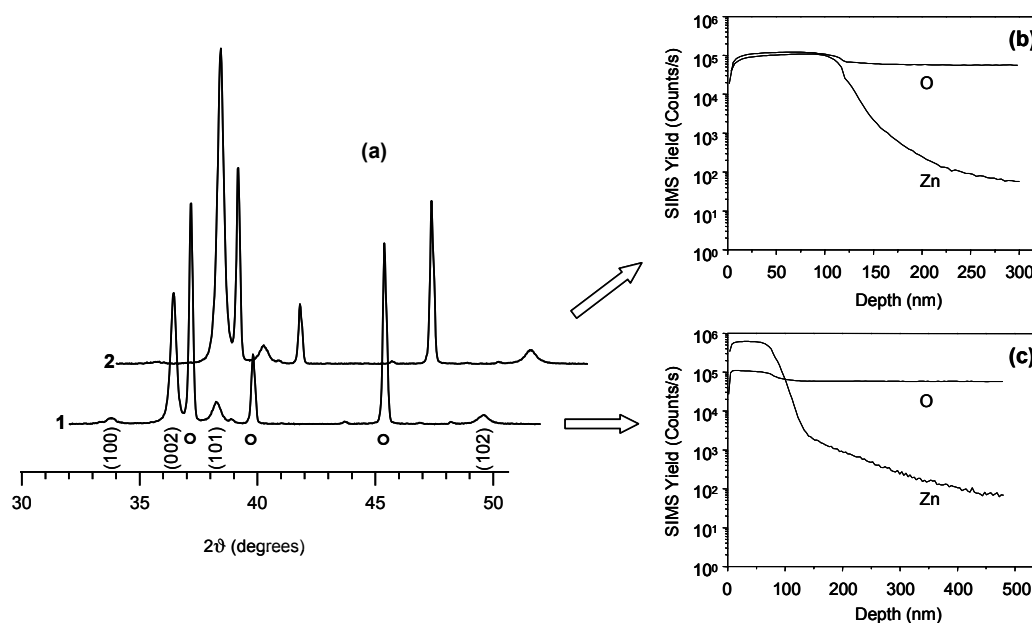


Fig. S1 a) GIXRD patterns of two representative ZnO specimens characterized by a different thickness (1: 78 nm; 2: 116 nm). Reflections of the *wurtzite* phase are directly indexed, whereas diffraction peaks of the  $\text{Al}_2\text{O}_3$  substrate are marked by circles. SIMS depth profiles for samples 1 b) and 2 c).

AFM micrographs (Figs. S2) were obtained by a NT-MDT SPM Solver P47H-PRO instrument operating in tapping mode and in air. Images were recorded on different sample areas in order to check surface homogeneity. RMS roughness values were calculated after background subtraction through plane fitting.

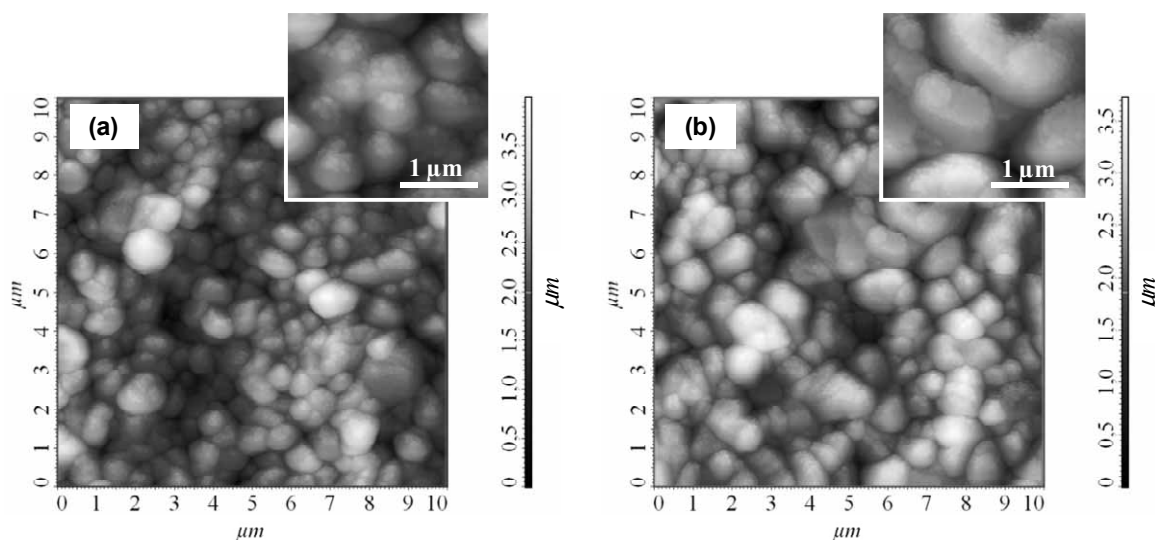


Fig. S2  $10 \times 10 \mu\text{m}^2$  AFM micrographs for two representative ZnO specimens with different thickness [a), 1: 78 nm; b), 2: 116 nm].

Field emission-scanning electron microscopy (FE-SEM) measurements were carried out at acceleration voltages between 5.0 and 20.0 kV by means of a Zeiss SUPRA 40VP instrument, equipped with an Oxford INCA x-sight X-ray detector for energy dispersive X-ray spectroscopy (EDXS) analyses. The mean nanoaggregate sizes were evaluated through the SmartSEM™ software.

For sensing measurements, two Pt interdigitated electrodes were deposited by sputtering with shadow masking on the specimen surface (spacing between electrodes = 190  $\mu\text{m}$ ). The sensor operating temperature was set by keeping constant the resistance of a platinum heater, deposited on the backside of  $\text{Al}_2\text{O}_3$  substrates ( $3 \times 3 \text{ mm}^2$ ; thickness = 250  $\mu\text{m}$ ), and calibrated using an IR camera in order to control its temperature coefficient. Gas sensing tests were performed by means of the flow-through technique<sup>S3-S5</sup> using a constant synthetic air flow ( $0.3 \text{ l} \times \text{min}^{-1}$ ) as carrier gas for the target analyte dispersion. The sensing element was inserted in a standard socket into the analysis chamber, maintained at 20°C, atmospheric pressure and constant humidity level (40%). Tests were carried out by the volt-amperometric technique at a constant bias of 1 V, registering

the flowing current by means of a picoammeter (Keithley 486) and a multiplexer (Keithley 7001 SWITCH SYSTEM). Before measurements, all samples were pre-stabilized at the working temperature for 8 h. The sensor response was defined as the relative conductance (resistance) variation upon exposure to reducing (oxidizing) target gases, respectively.<sup>S3,S4,S6-S14</sup>

Table S1 reports the fitting parameters obtained for the tested gaseous analytes at different working temperatures.

Table S1. Representative parameters obtained by best fitting of the calibration curves  $R = A \times [C]^N$  for the tested analytes.

Gas	Temperature (°C)	A	N
Ethanol	400	24.9	0.2
Acetone	200	1.18	0.19
Ozone	200	45.3	0.07
Nitrogen dioxide	100	18.6	0.6

#### Notes and references

- S1 D. Barreca, A. Gasparotto, E. Tondello, C. Sada, S. Polizzi and A. Benedetti, *Chem. Vap. Deposition*, 2003, 9, 199.
- S2 D. Bekermann, D. Rogalla, H. -W. Becker, M. Winter, R. A. Fischer, A. Devi, *Eur. J. Inorg. Chem.*, 2010, 1366.
- S3 E. Comini, G. Faglia, M. Ferroni and G. Sberveglieri, *Appl. Phys., A*, 2007, 88, 45.
- S4 G. Sberveglieri, C. Baratto, E. Comini, G. Faglia, M. Ferroni, A. Ponzoni and A. Vomiero, *Sens. Actuators, B*, 2007, 121, 208.
- S5 D. Barreca, A. Gasparotto, C. Maccato, E. Tondello, E. Comini and G. Sberveglieri, *Nuovo Cimento Soc. Ital. Fis., B*, 2008, 123, 1369.
- S6 J. Y. Park, S. -W. Choi and S. S. Kim, *Nanoscale Res. Lett.*, 2010, 5, 353.

- S7 B. S. Kang, Y. W. Heo, L. C. Tien, D. P. Norton, F. Ren, B. P. Gial and S. J. Pearton, *Appl. Phys., A*, 2005, 80, 1029.
- S8 Y. Liu, J. Dong, P. J. Hesketh and M. Liu, *J. Mater. Chem.*, 2005, 15, 2316.
- S9 E. Oh, H. -Y. Choi, S. -H. Jung, S. Cho, J. C. Kim, K. -H. Lee, S. -W. Kang, J. Kim, J.-Y. Yiun and S. -H. Jeong, *Sens. Actuators, B*, 2009, 141, 239.
- S10 D. Calestani, M. Zha, R. Mosca, A. Zappettini, M. C. Carotta, V. Di Natale and L. Zanotti, *Sens. Actuators, B*, 2010, 144, 472.
- S11 E. Comini, C. Baratto, G. Faglia, M. Ferroni, A. Vomiero and G. Sberveglieri, *Progr. Mater. Sci.*, 2009, 54, 1.
- S12 A. Z. Sadek, S. Choopun, W. Wlodarski, S. J. Ippolito and K. Kalantar-Zadeh, *IEEE Sens. J.*, 2007, 7, 919.
- S13 I. Kortidis, K. Moschovis, F. A. Mahmoud and G. Kiridiakis, *Thin Solid Films*, 2009, 518, 1208.
- S14 C. Baratto, G. Sberveglieri, A. Onischuk, B. Caruso and S. di Stasio, *Sens. Actuators, B*, 2004, 100, 261.